

Part2Whole: Iteratively Enrich Detail for Cross-Modal Retrieval with Partial Query

Guanyu Cai,* Lianghua He
Tongji University

Xinyang Jiang,† Jun Zhang, Yifei Gong, Pai Peng, Xiaowei Guo, Xing Sun
Tencent Youtu Lab

caiguanyu@tongji.edu.cn, xinyangj@zju.edu.cn

Abstract

Text-based image retrieval has seen considerable progress in recent years. However, the performance of existing methods suffers in real life since the user is likely to provide an incomplete description of a complex scene, which often leads to results filled with false positives that fit the incomplete description. In this work, we introduce the partial-query problem and extensively analyze its influence on text-based image retrieval. We then propose an interactive retrieval framework called Part2Whole to tackle this problem by iteratively enriching the missing details. Specifically, an Interactive Retrieval Agent is trained to build an optimal policy to refine the initial query based on a user-friendly interaction and statistical characteristics of the gallery. Compared to other dialog-based methods that rely heavily on the user to feed back differentiating information, we let AI take over the optimal feedback searching process and hint the user with confirmation-based questions about details. Furthermore, since fully-supervised training is often infeasible due to the difficulty of obtaining human-machine dialog data, we present a weakly-supervised reinforcement learning method that needs no human-annotated data other than the text-image dataset. Experiments show that our framework significantly improves the performance of text-based image retrieval under complex scenes.

1. Introduction

Recently, cross-modal retrieval, especially text-based image retrieval has gained increasing attention [38]. Although significant improvement has been achieved with existing methods [16, 38, 7] for text-based retrieval, we found

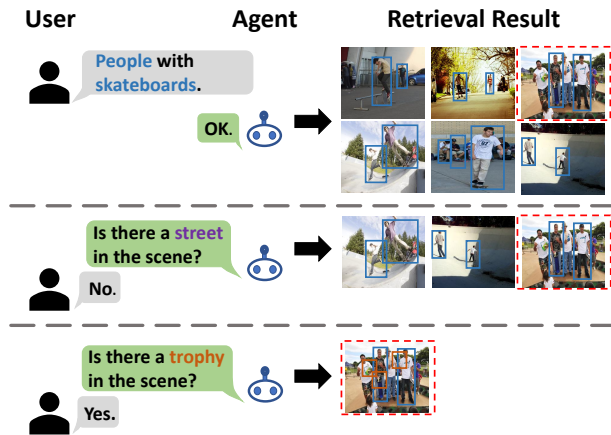


Figure 1: An illustration of Part2Whole. The agent enriches the textual query and narrows down the searching scope by iteratively asking users to confirm on more information. The target image is highlighted with red rectangle.

in practice their retrieval result is barely satisfactory when users only describe some local regions in a complex scene.

In this work, we introduce a new concept of *partial-query* problem in text-based image retrieval, where the initial text query only describes some objects in the target image. Studies [32, 30] have found that when examining a scene, people tend to only focus on the objects that stand out the most. This could lead to problems where the most identifiable objects in a scene are not the distinctive difference between the target image and similar candidates, thus making the user’s input insufficient for retrieving the target image. Existing text-based retrieval methods are mainly based on two mechanisms: local alignment and interactive retrieval. Both of them suffer from the partial-query problem. Specifically, local alignment methods [16, 5, 38] discover the partial relevance between the query and regions in the target image, but the lack of information in the query

*Work done during internship at Youtu Lab

†Corresponding author: Xinyang Jiang

pulls down the upper bound of performance. Pioneer interactive retrieval methods [6, 35, 28, 14, 12, 37, 7, 33] heavily rely on users’ manual feedback. They perform unsteadily because users usually lack an understanding of the retrieval model and the status of the images in the gallery to give optimal feedback. To help the user give better feedback, they usually give the user one or several candidate images for reference (i.e., the top K retrieved image with the partial query). However, with only partial queries, there is usually a large semantic gap between the reference and target image, which can hardly help the users to provide helpful feedback to improve the retrieval. Hence, cross-modal retrieval with partial queries remains a great challenge.

To tackle partial queries, we propose a novel interactive retrieval framework as shown in Figure 1. The agent first retrieves a set of relevant candidates from the gallery based on initial text queries. Then, the agent will analyze the retrieval results and the overall status of gallery, and select a differentiating object for users to confirm its presence. Based on users’ confirmation, the agent narrows down the range of candidates and eventually gathers enough information to locate the target image. In this framework, after providing the initial query, users are free from the burden of refining the details of the partial query, instead only need to confirm the existence of objects from the target image. Reinforcement learning is used to automatically obtain a policy to find the optimal objects that quickly distinguish the target image from the other candidates. This novel interactive retrieval process that iteratively enriches the details of partial query is called *Part2Whole*. Unlike previous interactive methods [7, 21] that require human-annotated dialogs which is impractical to widely collect, our Part2Whole framework is trained in a weakly-supervised manner, where only text-image pairs are needed.

The contributions of our framework are as follows: 1) To our knowledge, this is the first work that formally addresses and analyzes the problem of partial query in cross-modal retrieval. 2) Instead of heavily relying on the user to provide missing details, we propose a novel interactive retrieval framework *Part2Whole* that introduces an interactive agent to automatically select the most differentiating details for users to confirm. 3) Rather than using human-annotated dialogs, we propose a weakly-supervised reinforcement learning framework to optimize the interactive policy that explores the statistical characteristics of the gallery. Experiments show that our framework is effective and robust with partial queries.

2. Related Work

2.1. Text-based Image Retrieval

Most text-based image retrieval approaches are based on deep neural networks [38, 16, 18, 10, 34, 5]. The main ob-

jective of the retrieval system is to accurately measure the similarity between the inputs from two different modalities. Cross-Modal Projection Learning (CMPL) [38] is proposed to pull image and text embeddings into an aligned space. To further enhance the retrieval performance in a fine-grained way, [16, 18, 10, 34] proposed different attention-based approaches, applying visual attention between every image region and word.

2.2. Query Expansion

Query expansion also deals with incomplete information in retrieval. Different from our work which handles partial queries that are complete sentences of local regions, it focuses on queries that are incomplete sentences. An incomplete sentence as the query leads to poor retrieval. Thus, query expansion methods are proposed [39, 19, 23, 4, 9]. In the text search field, [39] learns every user’s searching history to generate personalized expansion words. [19] explores query expansion by calculating similarity distance in thesaurus indexed collections. Other methods focus on image or video retrieval [23, 4, 9]. Gallery images or videos are first classified by its concept. Then, systems provide expansion based on a knowledge base. These query expansion methods are purely text-based instead of cross-modal. Although some methods [23, 4, 9] are used to retrieve visual contents, they also need text descriptions of contents first and then apply text-based methods to expand queries.

2.3. Visual Dialog

Visual dialog is another intriguing task aiming to let the machine understand the visual content and have a natural conversation with the user about it. After examining the image, the agent can answer the user’s questions on different aspects. Mainstream approaches are based on policy-based reinforcement learning to achieve good question-answer performance [25, 2, 3]. However, the dialogs are purely text-based for both the questioner and answer agent, and a manually annotated dialog dataset is needed to train a visual dialog system.

2.4. Interactive Image Retrieval

It is often hard for the retrieval model to locate the target image with the initial query. Inspired by visual dialog, interactive image retrieval systems [35, 28, 14, 13, 12, 26] are proposed to solve this problem. In these systems, users can give feedback to an agent according to a reference image. There are two types of feedback: relevance and difference. For the former one [35, 28], users give relevance judgment for the current retrieval results. Then the system re-ranks its retrieval results next round by linking high-level concepts and low-level features from the user’s feedback. For the latter one [14, 13, 12, 26], users tell the difference between the reference image and the target image to the system. The

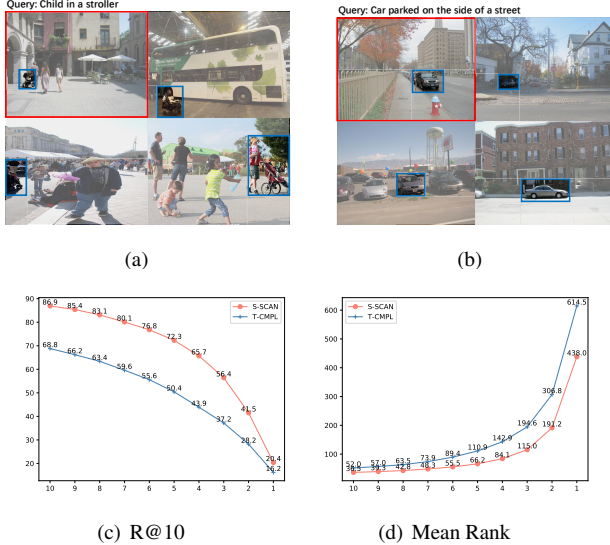


Figure 2: Effect of partial queries. (a) and (b) are visualizations of partial-query retrieval for complex scenes. The target image is surrounded with a red box and the others are the top three ranked scenes. The region that matches the query is surrounded with a blue box. (c) and (d) demonstrates R@10 and Mean Rank of a retrieval model as queries decrease. The horizontal axis represents the query number.

system then whittles away the irrelevant images and ranks the correct one to the top. Due to the diversity of scenes, different approaches are proposed for different fields. Based on the feedback on the detailed attributes, [36] achieves remarkable results on CelebA [20]. Analogously, [7, 17] focus on the fashion domain and achieve more effective retrieval results.

3. Problem Statement

In this section, we define the partial-query problem and explore its effects on cross-modal retrieval from both intuitive and quantitative views. For text-based image retrieval, a set of captions $Q = \{q_n\}_{n=1}^{N_Q}$ composes the complete description of a scene i , where each q_n describes a region. By regarding Q as queries, the goal of a retrieval model R is to retrieve the target image i_* from a gallery $I = \{i_j\}_{j=1}^N$. The partial-query problem considers that only a subset of Q , i.e. $Q_p = \{q_n\}_{n=1}^{N_p}$, $N_p \leq N_Q$, is given to R . With limited information in Q_p , i_* is hard to locate correctly.

To provide an intuitive view of the partial-query problem, Figure 2 (a) and (b) shows two examples of a cross-modal retrieval model’s results given partial queries. In both examples, the target scene ranks lower than 1000th, while the top three ranked scenes are false positives. We observe that a common object (indicated by blue boxes) described by the query is present in both target image and top-3 false

positives. However, besides the common object, the rest of the scenes are vastly different. For example, in Figure 2 (a), besides the stroller mentioned in the query, the target scene consists of umbrellas, chairs, and so on. Whereas the others consist of different objects like trees and buses. If the retrieval model receives a complete description including all objects, existing methods [16, 18, 34] would perform excellently. Due to the partial query focuses only on a single region therefore lacking differentiating information, many scenes may fit its description thus become false positives. Therefore the performance of traditional retrieval models collapses when facing the partial-query problem.

To excavate the quantitative effects of partial queries, we implement two text-image retrieval models, S-SCAN and T-CMPL, modified from SCAN [16] and CMPL [38]. The implementation is detailed in Section 5. Visual Genome [15] is used to quantitatively evaluate the influence of partial queries on retrieval performance. For each image, its complete description includes 10 captions for different regions. We gradually decrease the number of captions and use these captions as partial queries to retrieve the target image. R@10 and Mean Rank (MR) are adopted to measure performance. As shown in Figure 2 (c) and (d), for both models, R@10 decreases and MR increases as the degree of incompleteness increases. Even when only 1 caption is given, R@10 drops off more than 50% drastically for both models. These results reveal that partial queries harm the retrieval performance heavily and the more partial the queries, the worse the retrieval.

4. Method

4.1. Discovery and Assumption

It is intuitive that partial queries hardly retrieve the target scene because of its limited information. However, we discover that some cost-free information is always ignored. In detail, most text-image matching methods [16, 18, 34] extract image features by an object detector [1], but they never leverage the ready-made information of object categories. Another discovery is that the distribution of object categories is not uniform. Some objects, such as “trophy” and “skateboard”, rarely appear in scenes. If a scene includes these objects, they are discriminative enough to narrow down the searching scope quickly. The two discoveries inspire us that objects in a scene can be auxiliary information to compensate for the effect of partial queries.

As a result, the aforementioned discoveries inspire us that exploring objects in a scene could be an effective way to enrich the detail of a partial query. To verify how the effectiveness of adding object descriptions into the partial query retrieval system, we explore the upper bound of our discoveries by assuming *Objects in the target scene are knowable*.

Specifically, we compare the retrieval performance of

Method	R@1	R@5	R@10	MR
S-SCAN	4.5	13.6	20.4	416.0
S-SCAN+Objects	46.4	70.2	78.4	28.4

Table 1: Retrieval improvements over a basic text-image matching model with ground-truth object descriptions.

entering only one partial query to a model against entering one partial query and its corresponding object descriptions. As shown in Table 1, remarkable improvements are achieved by adding ground-truth object descriptions where R@10 is improved by 58%, and MR is moved up about 400. The prominent enhancements verify that our discoveries are helpful to the retrieval under the proposed assumption.

4.2. Interactive Retrieval Agent

In reality, the upper bound in Section 4.1 is very difficult to achieve, because the agent never know what objects are in the target image. Hence, we propose an interactive retrieval system to obtain the object information through T rounds of interactions with the user.

However, directly letting users provide object information brings unstable retrieval results, because users lack an understanding of the object distribution in gallery to choose discriminative objects. Hence, we propose to let the AI agent analyzes the distribution in gallery and offers object candidates to users as hints during interactions. Users simply feedback to the agent whether these object candidates are in the target scene or not. This type of interaction also reduces the burden of users where users just need to choose several options in the candidates instead of manually giving text or relevance feedback like previous interactive retrieval [7, 21, 35]. After obtaining objects from users, two strategies are conducted to facilitate the retrieval: (1) adding text descriptions of objects in the target scene as coarse-grained queries, (2) regarding scenes containing objects excluded in the target scene as negative samples.

To elaborate on the interactive process, we first define some notations, then describe four components that constitute the agent as shown in Figure 3, finally illustrate the whole workflow. At t th round, the input partial queries are denoted as $Q_t = \{q_n\}_{n=1}^{N_Q^t}$ where q_n denotes a partial query. An image i_t selected from the retrieval gallery $I = \{i_n\}_{n=1}^N$ where N is the number of all images and a set of object candidates $A_t = \{a_n\}_{n=1}^{N_A}$, $a_n \in \mathcal{A}$ is provided to users where \mathcal{A} is a set of all objects. The objects present in the target scene are defined as positive objects, denoted as $A_t^p = \{a_n^p\}_{n=1}^{N_A^p}$. The objects not present in the target image are defined as negative ones, denoted as $A_t^q = \{a_n^q\}_{n=1}^{N_A^q}$ where $N_A^q + N_A^p = N_A$. The four components are detailed as follows.

Text Encoder. The Text Encoder TE embeds partial

queries into a textual-visual feature space. To obtain a set of textual features $X_t^T = \{x_n^T\}_{n=1}^{N_Q^t}$, $x_i^T \in \mathbb{R}^D$ in each round, we apply a gated recurrent unit to all partial queries as [31] where $x_n^T = TE(q_n)$, $q_n \in Q_t$.

Image Encoder. The Image Encoder IE extracts visual features $\mathcal{X}^I = \{X_n^I\}_{n=1}^N$, $X_n^I \in \mathbb{R}^{36 \times D}$ from all gallery images and predicts a set of objects $\{a_j\}$, $a_j \in \mathcal{A}$ in each scene i_n , denoted as A_n . We denote the process as $(X_n^I, A_n) = IE(i_n)$.

Ranker. The Ranker takes charge of retrieving the target scene according to X_t^T , \mathcal{X}^I , A_t and A_n .

Candidate Generator. At each round, the Candidate Generator selects the most differentiating Object candidates A_t for users to confirm. The confirmed object information is used to enrich the details in partial query and rule out candidate images contain negative objects.

The whole interactive workflow is illustrated in Figure 3. At each iteration t , given the partial queries Q_t , the Text Encoder embeds Q_t into textual features X_t^T and the Image Encoder extracts visual features \mathcal{X}^I and predicts objects A_n in each scene. Then, the Candidate Generator selects a set of differentiating object candidates A_t for users to confirm. Users choose positive objects A_t^p in the target scene and negative objects A_t^q are also determined. Similar to common text-based retrieval methods [38, 16], the Ranker computes similarity $S_{t,n}(X_t^T, X_n^I)$ between X_t^T and X_n^I firstly. However, our method will further refine the similarities of query containing negative objects by $S_{t,n} = S_{t,n} \times 0.9$, if $A_n \cap A_t^q \neq \emptyset$ and an image i_t is provided to users. For the next round of text-image retrieval, the partial queries are updated by adding the positive objects $Q_{t+1} = Q_t \cup A_t^p$. Then the four components conduct the same operations as above. This process continues until the target scene is selected or t reaches T .

4.3. Weakly-supervised Policy Learning

Manually defining a criterion for the Candidate Generator to select a ‘‘good’’ object is difficult, so we propose an RL based policy learning approach that automatically finds an optimal policy by letting the Candidate Generator iteratively interact with the interactive retrieval agent and self-update based on the system’s feedback.

The whole policy learning is very simple and can be easily conducted in a weakly-supervised manner, because we only need to know objects in each scene and users’ behavior can be mimicked by ground-truth objects in the target scene. We can even just reuse the detector for extracting image features to detect objects. On the contrary, previous dialog-based retrieval methods [7, 21, 3] require burdensome collections of chatting sessions. The superiority that our method needs no extra data collections makes it more practical.

Reinforcement Learning. The policy obtained by the

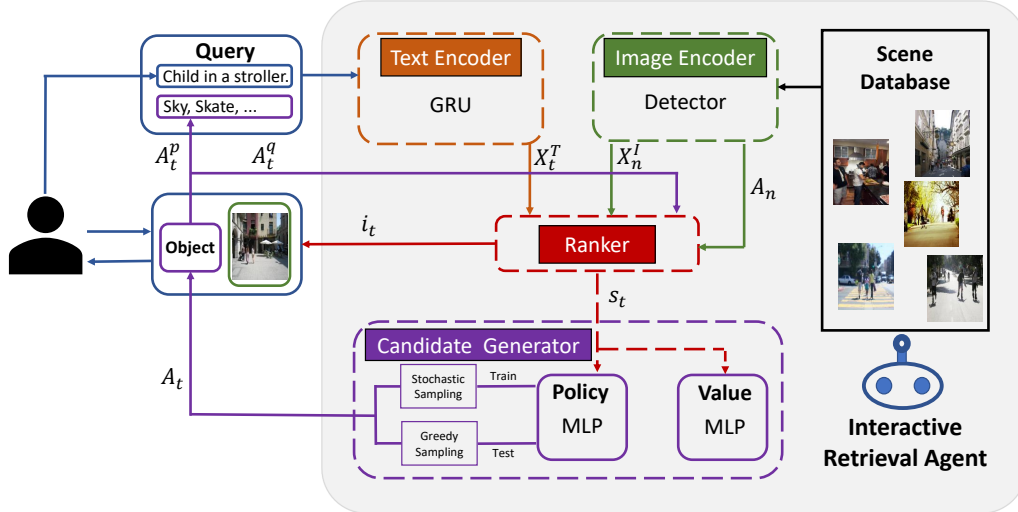


Figure 3: The proposed interactive cross-modal retrieval framework of Part2Whole. The interactive retrieval agent gradually enriches details of a scene by heuristically providing users with object candidates.

Candidate Generator is modeled as a policy net π , parameterized with ϕ_π , which outputs each object’s probability $P(a)$ of getting selected. The five components in our policy learning framework *action*, *state*, *policy*, *value* and *reward* are as follows:

Actions refers to the objects selected by the Candidate Generator at each round, i.e., $a \in \mathcal{A}$.

State s^t is defined as a concatenation of $s_1^t = \sum_{n=1}^{N_Q^t} x_n^T / N_Q^t$ and $s_2^t = P_r(a)$, where $P_r(a)$ is the distribution of a among the top 100 scenes generated by the Ranker. We utilize such design to make π aware of information both from partial queries and the ranking list.

Reward is defined as the similarity between textual features in each round and the target visual feature, i.e., $S(X_t^T, X_*^I)$ where X_*^I is the visual feature of the target scene.

Policy π is implemented with a three-layer MLP. The object sampling distribution $P(a)$ is approximated with $\pi(s^t)$.

Value is estimated with $V(s^T)$. The value net V is implemented with a two-layer MLP, parameterized with ϕ_v .

Given the actions, state, reward, value and policy, a Proximal Policy Optimization (PPO) [29] is applied to optimize the policy net ϕ_π and ϕ_v . Please refer to the original paper of PPO for more details.

Shaping. RL is easily stuck with sparse rewards [24], thus, previous RL-based dialog agents [7, 25, 3] adopt a supervised learning for shaping the RL training. However, since we try to avoid an extra collection of real-world dialogs, we propose a novel shaping method guided by a joint distribution of query and object. Inspired by word2vec [22] that words are related if they always occur simultaneously, there is also a high probability for an object to be semantically relevant to the queries if they describe the same scene.

Intuitively, an object relevant to the query is more likely to be a positive object of the target image, which could potentially move the target up the rank-list by a lot. Thus, the Candidate Generator should focus more on this type of objects. To adopt this intuition to policy learning, we first obtain the conditional probability $P(a|Q_t)$ of an object relating to a query by counting the frequency of the tokenized words $\{w_n\}_{n=1}^{N_w}$ occur in different queries, as follows:

$$f_{n,j}(w_n, a_j) = \sum_{k=1}^N \mathbb{1}(w_n \in i_k | a_j \in i_k) \quad (1)$$

where $a_j \in \mathcal{A}$ and $\mathbb{1}(\cdot)$ is an indicator function. $w_n \in i_k$ means that w_n occurs in a description of i_k and $a_j \in i_k$ denotes an object in i_k . Thus, $P(a_j|Q_t)$ is estimated with

$$P(a_j|Q_t) = \frac{\sum_{w_n \in Q_t} f_{n,j}(w_n, a_j)}{\sum_{j=1}^{|\mathcal{A}|} \sum_{w_n \in Q_t} f_{n,j}(w_n, a_j)} \quad (2)$$

where $w_n \in Q_t$ denotes w_n occurs in any query in Q_t . Guiding with the statistics, We then train π by optimizing

$$\mathcal{L}_s = \sum_{t=1}^{N_s} (P(a|Q_t) - \pi(s^t))^2 \quad (3)$$

where N_s means that \mathcal{L}_s is optimized for every N_s rounds.

Therefore, loss of the policy learning process is $\mathcal{L} = \mathcal{L}_p + \alpha \cdot \mathcal{L}_s$, where coefficient α is used to balance the RL learning and shaping.

5. Experiments

Dataset. There is no existing benchmark for interactive partial-query retrieval and we build a new dataset based on

Visual Genome [15]. In Visual Genome, multiple regions are detected by an object detector [1] for each image, and each of the object region is annotated with a textual description. We preprocess the data by following the protocol in [31], resulting in 105,414 image samples. Images are split into 92,105/5,000/9,896 for training/validation/testing. To perform an interactive partial-query retrieval without the challenge of extra data collection, we regard a region caption as a partial query offered by users and objects in the target image as feedback from users. All evaluations are performed on the test split.

Baselines. Part2Whole is a simple framework compatible to any cross-modal retrieval methods. In our experiments, we implement variants of SCAN [16] and CMPL [38], which are named Simplified SCAN (S-SCAN) and CMPL with Triplet loss (T-CMPL) respectively, as the basic retrieval models and build the proposed interactive retrieval agent on them. Both of the variants adopt the text and image encoder in Section 4.2 to obtain textual features $X^T = \{x_j^T\}_{j=1}^J, x_j^T \in \mathbb{R}^D$ and visual features $X^I = \{x_{k,m}^I\}_{k,m=1}^{K,M}, x_{k,m}^I \in \mathbb{R}^D$. (a) **S-SCAN:** We modify the bidirectional attention mechanism in SCAN to a unidirectional one to adopt multi-query inputs. Thus, the similarity between x_j^T and x_k^I is modified as

$$S_{j,k}(x_j^T, x_k^I) = \frac{1}{M} \sum_{m=1}^M \gamma_{j,k} \cdot \cos(x_j^T, x_{k,m}^I) \quad (4)$$

where $\gamma_{j,k} = \frac{\exp(\cos(x_j^T, x_{k,m}^I))}{\sum_{m=1}^M \exp(\cos(x_j^T, x_{k,m}^I))}$ and \cos denotes the cosine similarity. The similarity between X^T and X^I is the average of $S_{j,k}$ among all x_j^T and x_k^I . (b) **T-CMPL:** Similar to CMPL, we adopt global alignment to match textual and visual features without any attention mechanisms. Thus, the similarity between x_j^T and x_k^I is

$$S_{j,k}(x_j^T, x_k^I) = \cos(x_j^T, \frac{1}{M} \sum_{m=1}^M x_{k,m}^I) \quad (5)$$

The similarity between X^T and X^I is the average of $S_{j,k}$ among all x_j^T and x_k^I .

Both of S-SCAN and T-CMPL are optimized with a common ranking loss. These modifications mainly focus on similarity computing. They impose no effects on the interactive process, thus, we can verify the proposed interactive retrieval framework fairly.

Implementation Details. During training, T is set to 20 to conduct a twenty-round interaction. In each round, we set $N_A = 10$ which means sampling 10 objects from the object sampling distribution $P(a)$. During testing, we vary T and N_A and apply a greedy sampling to choose actions with the highest probabilities. Similar to [1], we utilize a Faster RCNN pretrained on Visual Genome with 1600 object categories to extract features of the top 36 regions and

Method	R@1	R@5	R@10	MR	Q	A
S-SCAN	4.5	13.6	20.4	416.0	1	10
S-SCAN+P2W	8.6	33.9	59.8	96.0	1	10
S-SCAN	14.7	31.8	41.7	166.7	2	5
S-SCAN+P2W	16.8	43.3	67.7	70.7	2	5
S-SCAN	33.5	56.2	65.9	59.0	4	3
S-SCAN+P2W	34.1	61.4	80.1	37.8	4	3

Table 2: Results of Part2Whole on S-SCAN after 10 rounds. P2W denotes the proposed Part2Whole framework.

Method	R@1	R@5	R@10	MR	Q	A
T-CMPL	3.1	10.5	16.3	593.4	1	10
T-CMPL+P2W	5.2	20.4	37.0	313.8	1	10
T-CMPL	7.3	19.5	28.3	283.3	2	5
T-CMPL+P2W	8.6	26.9	47.2	211.3	2	5
T-CMPL	14.5	33.5	44.0	118.2	4	3
T-CMPL+P2W	15.1	38.6	59.5	98.7	4	3

Table 3: Results of Part2Whole on T-CMPL after 10 rounds. P2W denotes the proposed Part2Whole framework.

predict objects of regions. Textual and visual features are mapped into vectors with a dimension of 256. For the optimization of policy learning, we update all parameters for every 600 rounds and adopt Adam [11] as the optimizer. Learning rates of ϕ_π, ϕ_v are $3e^{-4}$ and $1e^{-3}$. Coefficient α is set to 1000. All models are trained for 500 epochs.

Evaluation Metrics. We adopt the common R@K (K=1, 5, 10) metric and Mean Rank (MR) to measure the retrieval performance. R@K indicates the percentage of the queries where at least one ground truth is retrieved among the top-K candidates.

5.1. Results

Based on S-SCAN and T-CMPL, we build two interactive retrieval models with the proposed Part2Whole framework. To prove the effectiveness of Part2Whole, we test them in three settings: (1) Q1/A10, (2) Q2/A5, and (3) Q4/A3. QK means K queries are given by users in the beginning, and AK means K actions are provided by an agent in each round. All results are recorded after 10 rounds.

Results are illustrated in Table 2 and 3. For both basic retrieval models in three different settings, Part2Whole strengthens their performance in all evaluation metrics. Part2Whole enhances R@10 of S-SCAN from 20.4% to 59.8% and strengthens R@10 of T-CMPL by 20.7% with Q1/A3. In the other two settings, the advantage of R@10 brought from Part2Whole recedes a bit but at least achieves 14.2%. As for R@5, Part2Whole based on S-SCAN achieves 61.4% and the one based on T-CMPL achieves 38.6% with Q4/A3. In other settings, the enhancement of Part2Whole is more obvious and even achieves 11.5% with Q2/A5 based on S-SCAN. Both basic retrieval models are improved by Part2Whole of R@1 in all settings. In partic-

ular, Part2Whole based on S-SCAN achieves $R@1=34.1\%$ with Q4/A3. With Part2Whole, MR of both basic retrieval models in three settings is moved up by a large margin. These results demonstrate the effectiveness of Part2Whole.

5.2. Visualizations

Examples of interactive retrieval are shown in Figure 4. Several interesting discoveries are found out in visualizations. Firstly, the agent tends to offer several objects in the first few round regularly, such as “window”, “man”, “sky”, “head”, “tree” and so on. These are the objects that come up most frequently in Visual Genome¹. This is a reasonable choice because it either has a large possibility to add a ground-truth object to queries or eliminates plenty of images that include these objects. Secondly, the agent can offer objects that are not common but related to the semantics of given queries and images in latter rounds. For example, to retrieve the image that includes zebras, the agent offers “field” and “fence” in round 9 which rarely occur but are related to zebras. To retrieve the image with a query “White short sleeve shirt”, the agent offers “sunglasses” and “top” in round 5 which belong to clothing just like the query, and offers “car” which shows in the scene. We ascribe these properties to our policy learning approach. The statistic-based shaping guides the agent to give priority to the most frequent objects and the reinforcement learning promotes objects related to the semantics of scenes.

5.3. Ablation Studies

Number of Query and Action. To verify that our method is robust to the number of queries and actions, we test it based on S-SCAN with different query numbers $N_Q^1 \in \{1, 2, 4\}$ where users input 1, 2, or 4 queries and different action numbers $N_A \in \{3, 5, 10\}$ where the agent generates 3, 5, or 10 objects in each round. Results on $R@5$, $R@10$, and MR in each round are shown in Figure 5.

In detail, with the same queries, the performance Part2Whole gradually improves when N_A increases, which shows that more actions in each round facilitate the retrieval. On the other hand, when N_A is fixed, queries with higher $N_Q^1 = 4$ outperform the ones with lower N_Q^1 , which is consistent with our analysis in Section 3. Although models with fewer queries achieve worse performance, improvements over them are even more. Especially, when $N_Q^1 = 1$ and $N_A = 10$, Part2Whole achieves the largest improvement. We conclude that fewer queries leave more space for the agent to optimize the basic model’s retrieval. Despite the change of the number of queries and actions, Part2Whole consistently enhances S-SCAN on all metrics. It examines the robustness of Part2Whole which facilitates retrieval stably in all situations.

¹Statistics are given in https://visualgenome.org/data_analysis/statistics



Figure 4: Visualization of Part2Whole based on S-SCAN. We show examples in three settings. Ground-truth objects in each round are highlighted in red. The target image is surrounded with a red bounding box.

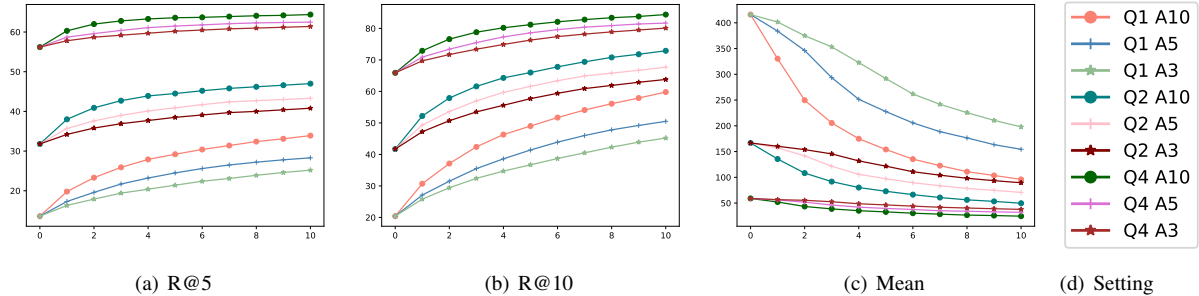


Figure 5: Results of Part2Whole based on S-SCAN. The horizontal axis represents the query turn. Q denotes the number of queries and A denotes the action number in each round.

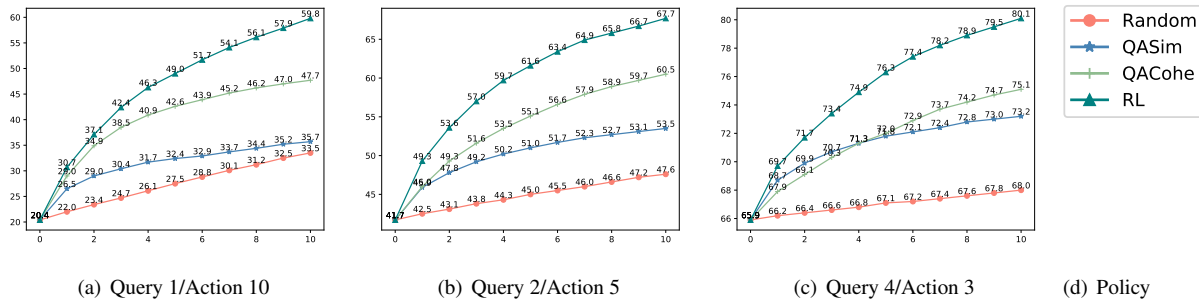


Figure 6: Results of different policies. The horizontal axis represents the query turn. The proposed RL-based policy learning approach outperforms the other policies.

Policy. Finding a policy that guides the agent to choose “better” objects is essential to Part2Whole. As a result, we compare our policy learning method with three pre-defined policies: (1) **Random**: In each round, the agent samples objects from a uniform distribution. (2) **QASim**: Inspired by [19], objects that have similar semantics with a query are preferred. We use cosine similarity between textual features of queries and objects to indicate their similarity. (3) **QACohe**: Considering that some objects tend to occur coherently, such as “building” and “window”, we compute a joint distribution $P_c(a_i, a_j)$ in the train split, where a_i and a_j are in the same image. Then, we use $P_c(a^*, a_j)$ where $a^* = \operatorname{argmax}_{a \in A} \frac{1}{N_Q^t} \sum_{n=1}^{N_Q^t} \cos(x_n^T, TE(a))$ to sample objects.

Experiments are conducted in three settings just like Section 5.1. As shown in Figure 6, under all settings, the proposed policy learning outperforms the other by a large margin in terms of R@10. After 10 rounds, our policy learning strategy outperforms the second-best policy by 12.1%, 7.2%, and 5.0% in three settings. We also observe that a good policy increases R@10 rapidly in the first several rounds and slows down in subsequent rounds. Such a policy provides better interactive experiences because users retrieve the target image with fewer interactions.

Model Agnostic. By comparing the improvements on S-SCAN and T-CMPL as shown in Table 4, we examine the proposed framework is model-agnostic. Although the

Method	R@1	R@5	R@10	MR	Q	A
T-CMPL+P2W	+1.9	+9.9	+10.7	-279.6	1	10
S-SCAN+P2W	+4.1	+20.3	+39.4	-320.0	1	10
T-CMPL+P2W	+1.3	+7.4	+8.9	-72.0	2	5
S-SCAN+P2W	+2.1	+11.5	+26.0	-96.0	2	5
T-CMPL+P2W	+0.6	+5.1	+15.5	-19.5	4	3
S-SCAN+P2W	+0.6	+15.2	+14.2	-21.1	4	3

Table 4: Results of Part2Whole on different basic retrieval models after 10 rounds.

implementation and performance of T-CMPL and S-SCAN are different, Part2Whole strengthens both of them on all evaluation metrics. In detail, the two models’ improvements of MR are very close. As for R@K metrics, improvements are more obvious on S-SCAN due to its better original performance. These results demonstrate that Part2Whole can easily cooperate with a common text-based retrieval model to boost the retrieval performance.

5.4. User Study

P2W is compared with Drill-Down (DD) [31] and WhittleSearch (WS) [14] that are re-implemented by us. 50 images are sampled from test set, and 4 different users search for each image with 3 methods for 5 rounds. The search performance in terms of R@1, R@5, R@10 and Mean Rank (Mean) are shown in Figure 7 a).

To evaluate user’s effort on different methods, we record

- bidirectional focal attention network for image-text matching. In *Proceedings of the 27th ACM International Conference on Multimedia*, pages 3–11, 2019.
- [19] Yongli Liu, Chao Li, Pin Zhang, and Zhang Xiong. A query expansion algorithm based on phrases semantic similarity. In *2008 International Symposiums on Information Processing*, pages 31–35. IEEE, 2008.
- [20] Ziwei Liu, Ping Luo, Xiaogang Wang, and Xiaoou Tang. Deep learning face attributes in the wild, 2015.
- [21] Sho Maeoki, Kohei Uehara, and Tatsuya Harada. Interactive video retrieval with dialog. In *Proceedings of the IEEE/CVF Conference on Computer Vision and Pattern Recognition Workshops*, pages 952–953, 2020.
- [22] Tomas Mikolov, Ilya Sutskever, Kai Chen, Greg S Corrado, and Jeff Dean. Distributed representations of words and phrases and their compositionality. In *Advances in Neural Information Processing Systems*, pages 3111–3119, 2013.
- [23] Apostol Natsev, Alexander Haubold, Jelena Tešić, Lexing Xie, and Rong Yan. Semantic concept-based query expansion and re-ranking for multimedia retrieval. In *Proceedings of the 15th ACM international conference on Multimedia*, pages 991–1000, 2007.
- [24] Andrew Y Ng, Daishi Harada, and Stuart Russell. Policy invariance under reward transformations: Theory and application to reward shaping. In *ICML*, volume 99, pages 278–287, 1999.
- [25] Aishwarya Padmakumar and Raymond J Mooney. Dialog policy learning for joint clarification and active learning queries. *arXiv preprint arXiv:2006.05456*, 2020.
- [26] Devi Parikh and Kristen Grauman. Relative attributes. In *2011 International Conference on Computer Vision*, pages 503–510. IEEE, 2011.
- [27] Shaoqing Ren, Kaiming He, Ross Girshick, and Jian Sun. Faster r-cnn: Towards real-time object detection with region proposal networks. In *Advances in Neural Information Processing Systems*, pages 91–99, 2015.
- [28] Yong Rui, Thomas S Huang, Michael Ortega, and Sharad Mehrotra. Relevance feedback: A power tool for interactive content-based image retrieval. *IEEE Transactions on Circuits and Systems for Video Technology*, 8(5):644–655, 1998.
- [29] John Schulman, Filip Wolski, Prafulla Dhariwal, Alec Radford, and Oleg Klimov. Proximal policy optimization algorithms. *arXiv preprint arXiv:1707.06347*, 2017.
- [30] Sarah Shomstein and Steven Yantis. Control of attention shifts between vision and audition in human cortex. *Journal of Neuroscience*, 24(47):10702–10706, 2004.
- [31] Fuwen Tan, Paola Cascante-Bonilla, Xiaoxiao Guo, Hui Wu, Song Feng, and Vicente Ordonez. Drill-down: Interactive retrieval of complex scenes using natural language queries. In *Advances in Neural Information Processing Systems*, pages 2651–2661, 2019.
- [32] Alex HC van der Heijden. *Selective Attention in Vision*. Routledge, 2003.
- [33] Nam Vo, Lu Jiang, Chen Sun, Kevin Murphy, Li-Jia Li, Li Fei-Fei, and James Hays. Composing text and image for image retrieval-an empirical odyssey. In *Proceedings of the IEEE Conference on Computer Vision and Pattern Recognition*, pages 6439–6448, 2019.
- [34] Yaxiong Wang, Hao Yang, Xueming Qian, Lin Ma, Jing Lu, Biao Li, and Xin Fan. Position focused attention network for image-text matching. In *Proceedings of the Twenty-Eighth International Joint Conference on Artificial Intelligence, IJCAI-19*, pages 3792–3798. International Joint Conferences on Artificial Intelligence Organization, 7 2019.
- [35] Hong Wu, Hanqing Lu, and Songde Ma. Willhunter: Interactive image retrieval with multilevel relevance. In *Proceedings of the 17th International Conference on Pattern Recognition, 2004. ICPR 2004.*, volume 2, pages 1009–1012. IEEE, 2004.
- [36] Xinru Yang, Haozhi Qi, Mingyang Li, and Alexander Hauptmann. From a glance to” gotcha”: Interactive facial image retrieval with progressive relevance feedback. *arXiv preprint arXiv:2007.15683*, 2020.
- [37] Aron Yu and Kristen Grauman. Fine-grained comparisons with attributes. In *Visual Attributes*, pages 119–154. Springer, 2017.
- [38] Ying Zhang and Huchuan Lu. Deep cross-modal projection learning for image-text matching. In *Proceedings of the European Conference on Computer Vision (ECCV)*, pages 686–701, 2018.
- [39] Z. Zhu, J. Xu, X. Ren, Y. Tian, and L. Li. Query expansion based on a personalized web search model. In *Third International Conference on Semantics, Knowledge and Grid (SKG 2007)*, pages 128–133, 2007.

7. Supplementary

7.1. Implementation Details

In this section, we describe implementation details of the parameterized components in Part2Whole: Text Encoder, Image Encoder, policy net, and value net.

Text Encoder. We map the natural language to a 256-dimensional vector space. Given a sentence T that contains n words, we represent the i th word in it with a one-hot vector showing the index of the word in a vocabulary and then embed the word into a 300-dimensional vector x_i through an embedding matrix W_e . Then, we use a one-layer unidirectional GRU to map the vector to the final textual feature along with the sentence context. The GRU reads the sentence T from 1 to n th word and obtains the final textual feature x^T :

$$x^T = GRU(x_i), i \in [1, n] \quad (6)$$

We do not use a bidirectional GRU in this work because the performance between them is close.

Image Encoder. Given an image I , we aim to map it to a set of 256-dimensional vectors $X^I = \{x_1^I, x_2^I, \dots, x_k^I\}$, $k = 36$ where each vector encode a region and predict a set of objects $A = \{a_1, a_2, \dots, a_j\}$ in an image. We refer to detection of salient regions as bottom-up attention [1] and implement it with a Faster-RCNN [27]. We adopt the Faster-RCNN whose backbone is a ResNet-101 [8] pretrained by Anderson et al. [1] on Visual Genome [15]. For each region i , f_i is defined as the mean-pooled feature from this region and the dimension of f_i is 2048. To get a 256-dimensional vector as textual vectors, we add an two-layer MLP to transform f_i to x_i^I :

$$x_i^I = MLP(f_i) \quad (7)$$

As for predicting objects, the original model predicts attribute classes and instance classes together to learn feature representations with rich semantic meaning. However, in our Part2Whole, we just need objects in an image. Hence, we re-train a two-layer MLP to predict the objects in I . After obtaining X^I , we concatenate all vectors into a 36×256 -dimensional vector X_1^I and use the MLP to predict every object’s probability of being in I . The architecture of the re-trained MLP is shown in Table 5.

Policy Net. Given a state $s \in \mathbb{R}^{3202}$. The policy net π outputs a 1601-dimensional vector as the object sample distribution. During training, we apply a stochastic sampling to choose objects to users while in the testing period, a greedy sampling is applied. The architecture of π is shown in Table 6.

Value Net. Given a state $s \in \mathbb{R}^{3202}$. The value net V outputs a scalar that estimates the real advantage returned by the interactive agent. According to [29], estimating the advantage is helpful to reduce the variance of reinforcement learning. The architecture of V is shown in Table 7.

Type	Weight shape	Input size
Fc	2048×256	$N \times 2048$
Fc	256×256	$N \times 256$
Fc	9216×256	$N \times 9216$
Fc	256×1601	$N \times 256$

Table 5: The architecture of MLP that predicts the objects in an image. N denotes the batchsize and Fc denotes the fully-connected layer.

Type	Weight shape	Input size
Fc	3202×256	$N \times 3202$
Tanh	-	$N \times 256$
Fc	256×256	$N \times 256$
Tanh	-	$N \times 256$
Fc	256×1601	$N \times 256$
Softmax	-	$N \times 1601$

Table 6: The architecture of policy net. Tanh denotes the hyperbolic tangent function and Softmax denotes the softmax function.

Type	Weight shape	Input size
Fc	3202×256	$N \times 3202$
Tanh	-	$N \times 256$
Fc	256×1	$N \times 256$

Table 7: The architecture of value net.

7.2. Pseudo Code

To describe our Part2Whole in more detail, we give the pseudo code of the whole workflow of Part2Whole as shown in Algorithm 1.

Algorithm 1 The whole workflow of Part2Whole

Initialize Text Encoder TE and Image Encoder IE
Initialize policy parameters ϕ_π and value parameters ϕ_V
Input: $I = \{i_n\}_{n=1}^N$: the whole gallery images
for episode=1,M **do**
 Input: i_* : the target image
 Input: $Q_1 = \{q_n\}_{n=1}^{N_Q^1}$: a set of input partial queries
 for $t=1, T$ **do**
 for $n=1, N_Q^t$ **do**
 $x_n^T = TE(q_n)$
 end for
 Obtain textual features $X_t^T = \{x_n^T\}_{n=1}^{N_Q^t}$
 for $n=1, N$ **do**
 $(X_n^I, A_n) = IE(i_n)$
 Compute similarity $S_{t,n}(X_t^T, X_n^I)$
 end for
 Question: Object candidates: $A_t = \{a_n\}_{n=1}^{N_A}$
 Feedback: Positive objects: $A_t^p = \{a_n^p\}_{n=1}^{N_A^p}$
 Feedback: Negative objects: $A_t^q = \{a_n^q\}_{n=1}^{N_A^q}$
 for $n=1, N$ **do**
 Refine $S_{t,n} = S_{t,n} \times 0.9, \text{ if } A_n \cap A_t^q \neq \emptyset$
 end for
 Output: $i_t = \operatorname{argmax}_{i_n} S_{t,n}$
 Update queries $Q_{t+1} = Q_t \cup A_t^p$
 end for
if episode % $N_s == 0$ **then**
 Collect a set of episode
 Run PPO to optimize ϕ_π and ϕ_V
end if
end for

7.3. Visualizations

In this section, we provide more visualizations of Part2Whole based on SCAN [16] to verify the effectiveness of it. We perform Part2Whole in three settings: (1) Q1/A10, (2) Q2/A5, and (3) Q4/A3. QK means K queries are given by users in the beginning, and AK means K actions are provided by an agent in each round. In detail, we visualize Part2Whole with Q1/A10, Q2/A5, Q4/A3 in Figure 8, 9 and 10, respectively.



child in a stroller
Rank: 1173

Round 1: Window, Sky, Person, Building, Man, Head, Shirt, Hand, Wall, Grass Rank: 119



Round 3: Shadow, People, Face, Clouds, Line, Leg, Road, Fence, Arm, Olives Rank: 10



fourescent porch
lighting of an white
three story building
Rank: 810

Round 1: Window, Tree, Head, Person, Ground, Man, Shirt, Hair, Wall, Grass Rank: 318



Round 3: Door, Road, Pants, Line, Fence, Traffic sign, Car, Front window, Olives, People Rank: 61



Round 8: Weeds, Umbrella, Mouth, Cap, Mantle, Hands, Baseboard, Foot, Roof, Clock Rank: 6



person on the boat
Rank: 778

Round 1: Man, Shirt, Head, Window, Sky, Person, Hand, Hair, Wall, Grass Rank: 453



Round 3: Building, Field, Floor, Hat, Table, Jacket, Light, Chair, People, Trees Rank: 39



Round 6: Water, Boy, Cap, Post, Lights, Foot, Sunglasses, Bag, Lady, Tail Rank: 3



Figure 8: Visualizations of Part2Whole based on SCAN with Query1/Action10.



two people walking a dog.
red-haired woman looking down.

Rank: 56

Round 1: Person, Hair, Sign, Man, Shirt

Rank: 17



Round 3: Building, Sign, People, Fence, Jacket

Rank: 4



bag of oranges.
green canvas bag on ground.

Rank: 18

Round 1: Ground, Man, Person, Shirt, Window

Rank: 2



a red and white carton of milk.
a white plastic knife.

Rank: 34

Round 1: Shirt, Hair, Sky, Man, Person

Rank: 2



Figure 9: Visualizations of Part2Whole based on SCAN with Query2/Action5.



Round 1: Sky, Ground, Man

Rank: 84



the street is grey.
the sidewalk.
marks on the sidewalk.
a car in the street.

Rank: 153

Round 3: Building, Tree, Grass

Rank: 10



Round 2: Sky, Building, Wall

Rank: 42



a very thick grey tree.
large brown mulchy area
around a grey tree.
side of a tan brick
building near a mulch bed.
top of a white umbrella.

Rank: 50

Round 4: Window, Hair, Sign

Rank: 9



Round 1: Shirt, Man, Person

Rank: 3

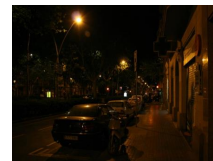


brown bowling ball
going down the lane.
man throwing a
bowling ball.
bowling pins at the end
of the lane.
lanes in the bowling
alley.

Rank: 57

Round 4: Sign, Head, Window

Rank: 15



a car on a street.
a window on a building.
this is a city street.
this is a car.

Rank: 58

Round 5: Light, Hair, People

Rank: 2



Figure 10: Visualizations of Part2Whole based on SCAN with Query4/Action3.